

## Introducing “*The Integrator*”: A novel technique to monitor environmental flow systems

Ricardo González-Pinzón <sup>1,\*</sup> Jancoba Dorley,<sup>1</sup> Peter Regier,<sup>1</sup> James Fluke,<sup>1</sup> Kelsey Bicknell,<sup>1</sup> Justin Nichols,<sup>1</sup> Aashish Khandelwal,<sup>1</sup> Emily Wolf,<sup>1</sup> Sarah N. Caruana,<sup>1</sup> David J. Van Horn<sup>2</sup>

<sup>1</sup>Department of Civil, Construction and Environmental Engineering, University of New Mexico, Albuquerque, New Mexico

<sup>2</sup>Department of Biology, University of New Mexico, Albuquerque, New Mexico

### Abstract

We introduce “*The Integrator*,” a novel technique to quantify transport and reaction metrics commonly used to characterize flow systems. This development consists of two products: (1) *The Integrator* sampling device and (2) its supporting mathematical framework, which is compatible with semi-continuous sensor data. The use of *The Integrator* device simplifies the logistics of sample collection and greatly reduces the number of samples needed, making it ideal to characterize systems that are: (1) difficult to access, (2) large and thus intractable or highly heterogeneous, and (3) highly instrumented otherwise but where a more holistic, mechanistic understanding may be gained by monitoring one or more currently untracked elements. We tested and validated *The Integrator* technique using experimental data collected from a heart rate monitor (high-quality, high-frequency data in response to known excitation events) and solute tracer experiments conducted in two contrasting (fourth and seventh order) rivers. In the Supporting Information, we provide details concerning the design of *The Integrator* device used in our field case studies and provide insight into potential improvements. Despite our case studies focus on the analysis of conservative and reactive transport of solutes in rivers, the principles behind *The Integrator* technique can be used to monitor water quality in hyporheic zones, aquifers, wetlands, swamps, karsts, oceans, wastewater treatment plants, pipe networks, and air quality. Furthermore, special arrangements of *Integrator* devices can be used to gather data at spatial and temporal resolutions that are currently unattainable due to high transportation and/or personnel costs.

Environmental monitoring of solutes (dissolved gasses, liquids, and solids) in flow systems is based on observations of concentrations that are relevant to the health of humans and ecosystems, and is typically done through sample collection organized either: (1) over time, at specific sites (Eulerian monitoring) and/or (2) across space (Lagrangian monitoring), within short-time windows (synoptic sampling) or seeking to follow a moving fluid parcel. Eulerian and Lagrangian monitoring allow estimates of control-volume, average responses of flow systems to upflow events (e.g., runoff from precipitation and plume propagation from spills) or tracer injections and can be done using grab or semi-continuous sampling (in situ automated sensors). Due to logistical simplicity, the use of

Eulerian monitoring to collect solute breakthrough curves (concentration vs. time) is much more common in environmental studies despite known challenges and faults (Nordin and Sabol 1974; Drummond et al. 2012; González-Pinzón et al. 2013) (Table 1), and Lagrangian approaches tend to be more used in modeling studies (e.g., particle-tracking analyses; Berkowitz and Scher 1995; Schumer et al. 2009) because dispersion and transient storage processes create wide distributions of travel times that are difficult to predict and respond to when tracking fluids in motion (Zhang et al. 1993, 2015; Goeury et al. 2014).

In tracer experiment studies done to understand the transport and fate of solutes, the most typical in situ faults that result in high uncertainty and errors are those related to the late beginning and/or the early cut-off of the sampling as they affect mass balances, the estimation of residence time distributions, and reactivity (Drummond et al. 2012; Wlostowski et al. 2017). Using experimental data, Govindaraju and Das (2007) showed that when the error in mass recovery is 16%, the errors in estimating the absolute temporal moments of solute breakthrough curves (i.e., the characteristic temporal responses of the flow

\*Correspondence: gonzaric@unm.edu

Additional Supporting Information may be found in the online version of this article.

This is an open access article under the terms of the Creative Commons Attribution License, which permits use, distribution and reproduction in any medium, provided the original work is properly cited.

**Table 1.** Typical needs, challenges, and faults in Eulerian monitoring of environmental systems.

Need	Challenges	In situ faults
Identify arrival and passage times	<ol style="list-style-type: none"> <li>1. It is difficult to identify the beginning and end of grab sampling campaigns tracking unobservable or low visibility solutes.</li> <li>2. In situ instruments may have detection limits above environmentally relevant concentrations, thus artificially lagging and/or truncating solute breakthrough curves.</li> </ol>	Breakthrough curves are started late and/or truncated prematurely, both of which affect mass, timing, variability, and skewness analyses.
Identify sampling frequency	<ol style="list-style-type: none"> <li>1. The forecasting of solute breakthrough curves relies on highly uncertain, nonphysical model parameters known to be discharge and site-specific.</li> <li>2. In situ, semi-continuous instruments may drift and/or generate false positives/negatives, which may affect the triggering and stoppage of automated (programmed) sampling.</li> </ol>	Grab samples with high information content (e.g., peak, inflection, and background) are not collected; conversely, high-frequency grab sampling and associated analytical costs may be unaffordable. In addition, semi-continuous sensors may miss the dynamics of rapid changing events due to coarse sampling frequencies.
Identify sampling coverage	<ol style="list-style-type: none"> <li>1. Defining sampling locations for grab and semi-continuous sampling relies on modeling forecasting, which may be highly uncertain.</li> <li>2. Spatial coverage is limited by availability of personnel or instrumentation at different sampling points.</li> <li>3. Capturing all possible end members affecting downflow responses is difficult or simply unattainable.</li> </ol>	The location of sampling points may not comply with the level of complexity of numerical models (e.g., violating mixing length assumptions in one-dimensional models) or lead to reaches that are either too short (e.g., where negligible reactions occur) or too long (e.g., outside of the range of sensor/analytical resolution).

system to a perturbation) can be as high as approximately  $(n + 1) \cdot 16\%$  for  $n = 0$  through  $n = 4$  (i.e., from 0<sup>th</sup> to 4<sup>th</sup>) order temporal moments. Even when the sampling begins and lasts the appropriate period to cover the full dynamic range of the time-series evolution, grab sampling analyses are challenged by the costs of sample collection and subsequent laboratory analyses, especially for spatially and/or temporally intense studies (e.g., repetitive fieldwork across river networks spanning months or years). For illustrative purposes, conducting tracer experiments to study scaling patterns in the transport and reactivity of solutes in a 1<sup>st</sup>–5<sup>th</sup> order fluvial network could require the processing of at least 20 Eulerian samples per monitoring site to describe solute breakthrough curves, totaling 200 samples if two monitoring sites are used per stream order. If, for example, ion chromatography was to be used, the cost of running the samples will conservatively reach USD \$2000 when filtration, transport, and analytical costs are included. Beyond such high costs, the sample processing time could easily surpass 125 nonstop working hours (assuming 25 min per sample, plus appropriate standards and blanks).

The advent of in situ monitoring sensors connected via telemetry has facilitated semi-continuous Eulerian monitoring of aquatic systems where sampling frequency can be varied automatically or remotely to capture relevant events such as rainfall, snowmelt, and wildfires (Bayard et al. 2005; Kraus et al. 2017; Melcher and Horsburgh 2017; Vaughan et al. 2017). However, grab sampling is still widely used, primarily due to lower upfront costs, but also to calibrate and validate in situ

sensors, as their reliability and accuracy present numerous challenges (e.g., drifting, miscalibration, false positives/negatives, and inability to detect low or high concentrations). In principle, grab sampling offers more flexibility than semi-continuous monitoring with respect to choosing sampling frequencies and coverage as decisions can be made on-the-go and personnel and transportation costs are typically smaller than instrument purchase, maintenance, and part-replacement costs. However, long-term monitoring may be onerous and much more expensive to do with grab sampling.

The logistical, technical, and affordability issues associated with grab and semi-continuous Eulerian monitoring have, and continue to, put a toll on the planning and execution of environmental studies. This increases the scientific gap in our understanding of the differences and similarities of eco-hydrological processes occurring within and across watersheds and, perhaps most importantly, across latitude, longitude, and elevation gradients around our planet. We highlight two examples of what is wrong with this status quo. First, ~ 90% of field tracer experiments done to estimate nutrient uptake in lotic ecosystems have been done in headwater streams (Tank et al. 2008; Hall et al. 2013; González-Pinzón et al. 2015), generating fundamental knowledge gaps regarding the mechanistic behavior of nutrient dynamics across fluvial networks, such as the role of physical characteristics, the impact of resource supply, quality, and stoichiometric constraints, and how all these factors vary over time and space, especially when considering anthropogenic disturbances. Second, a search of published studies on “stream” and “nutrient” across various geographic

regions (ISI Web of Science) showed a highly disproportionate concentration of studies in the Northern Hemisphere, despite the importance of intertropical and low-latitude ecosystems for local-to-planetary scale biogeochemical cycles (Riveros-Iregui et al. 2018). Therefore, we believe that by advancing current methods to conduct environmental monitoring of flow systems, we can improve our understanding of ecohydrology processes and open new ways of inquiring and testing research questions with emphasis on spatiotemporal variability.

This manuscript introduces “*The Integrator*,” a novel technique that simplifies grab sample collection and drastically reduces analytical costs, making it ideal to characterize systems that are: (1) difficult to access, (2) large and thus intractable or highly heterogeneous, and (3) highly instrumented otherwise but where a more holistic, mechanistic understanding may be gained by monitoring one or more currently untracked elements. We demonstrate that the mathematical framework that supports the use of *The Integrator* device is also compatible with semi-continuous monitoring. Therefore, our work coadvances grab and semi-continuous monitoring, making them analogous and comparable, which is ideal to reconcile and contrast data gathered across regions and continents. After presenting the mathematical framework that supports the use of *The Integrator* to quantify transport and reaction metrics commonly used to characterize flow systems, we validate the technique with experimental data collected from a heart rate monitor (high-quality, high-frequency data in response to known excitation events) and solute tracer experiments conducted in two contrasting (4<sup>th</sup> and 7<sup>th</sup> order) rivers.

### Conceptual and mathematical framework

A higher number of samples increases the temporal resolution in Eulerian monitoring. For grab sampling, the maximum resolution, precision, and accuracy will be achieved when the system’s response is captured continuously and uniformly (i.e., at a consistent sampling rate). If the sampling is continuous, the magnitude of the uniform sampling rate does not affect the information content since intensive (e.g., concentration) and extensive (e.g., mass) quantities scale proportionally with sample volumes. To demonstrate this principle, let us imagine that we sample the concentration of a solute in a river ( $C(t)$ ) continuously after a tracer is injected upstream at time  $t = 0$ , by simultaneously pumping water from the exact same monitoring site using two different but uniform pumping rates ( $q_1$  and  $q_2$ ). To facilitate the mathematical analysis, let us also assume that we put the sampled water inside two different, initially (at  $t = 0$ ) empty bottles, and continue to do this until  $t = t_f$  when the pumping and sample collection stop. The mass ( $M_1$  and  $M_2$ ) balance equations for such bottles will be:

$$M_1 = \int_{t=0}^{t=t_f} q_1 C(t) dt \quad (1a)$$

$$M_2 = \int_{t=0}^{t=t_f} q_2 C(t) dt \quad (1b)$$

Since the two pumping apparatuses are sampling the exact same flow system (i.e., simultaneously, at the same location and for the same duration), and the magnitudes of the solute fluxes across the sampling location (i.e., plume evolution) are only controlled upstream, the final concentrations of the solutes in the bottles ( $C_{f,1}$  and  $C_{f,2}$ ) must be exactly the same, regardless of their final volumes ( $V_1$  and  $V_2$ ), that is,

$$C_{f,1} = C_{f,2}; M_1/V_1 = M_2/V_2; M_1/q_1 = M_2/q_2 \quad (2)$$

Equations 1–2 introduce the working principle of *The Integrator*, a sampling technique that, to the best of our knowledge, has not been used to monitor environmental flow systems. *The Integrator* sampling is based on a simple device that continuously samples water from a flow system, down-flow of the perturbation or phenomena to be monitored. If *The Integrator* device is set to monitor an event before its arrival to the monitoring point, which does not necessarily need to coincide with the beginning of the perturbation (e.g., tracer injection), it can be used to quantify mass balances of conservative and reactive solutes from prearrival background to postpassage background, thus avoiding monitoring issues associated with late sample collection and early cut-off (cf. Table 1). In contrast to the ideal, composite sampling that can be achieved with *The Integrator*, traditional grab sampling used in environmental studies are not continuous (thus implicitly imperfect), though they may be uniform (equal time spacing between samples).

*The Integrator* device can be simply made using a pump, a filtration system and a storage container. For practical purposes, the pumping rate should be small (regardless of its magnitude, as demonstrated in Eqs. 1–2) to reduce the electrical power, ease the handling of sampled volumes, and to extend the life of all the parts used to pump and transport fluids (lower motions, pressures, and fluxes typically increase the life-span of all components). In the Supporting Information, we provide details concerning the design of *The Integrator* device that we used in our case studies (“Case studies” section), including a schematic and a list of parts used. In addition, we provide information on the development of several components that we optimized through experimentation (trial and error) and insight into potential improvements for future versions of *The Integrator* device. Next, we show the metrics that can be quantified with *The Integrator*.

### ***The Integrator: Reducing the complexity of flow systems to mass-balance analyses in bottles***

Fundamental time-series analyses of experimental concentration data can be done using low-order temporal moment analyses. The 0<sup>th</sup> temporal moment, which is the integral of the response over time, quantifies the overall response

strength to an excitation or perturbation of the flow system, and the 1<sup>st</sup> raw, normalized temporal moment provides information on the time between excitation and the characteristic response time of the system (Leube et al. 2012). These temporal moments estimated from experimental time-series can be matched with the theoretical temporal moments of transport and reaction models to estimate their parameters (Harvey and Gorelick 1995; Cunningham and Roberts 1998; Schmid 2003; Govindaraju and Das 2007; Das Bhabani et al. 2013; González-Pinzón and Haggerty 2013).

In Eulerian monitoring, the  $n^{\text{th}}$  raw (or absolute) moment,  $m_n$ , of an experimental concentration time-series,  $C(t)$ , is:

$$m_n = \int_0^\infty t^n C(t) dt \quad (3)$$

Raw temporal moments are related to statistical moments, but are applied to time rather than to random variables. The  $n^{\text{th}}$  normalized raw moment (or normalized absolute moment),  $m_n^*$ , is defined as:

$$m_n^* = \frac{m_n}{m_0} \quad (4)$$

Using experimental data, Eqs. 3, 4 can be computed as:

$$m_n = \sum_{k=1}^r \left( \frac{t_k + t_{k+1}}{2} \right)^n \left( \frac{C_k + C_{k+1}}{2} \right) (t_{k+1} - t_k) \quad (5a)$$

$$m_n^* = \frac{\sum_{k=1}^r \left( \frac{t_k + t_{k+1}}{2} \right)^n \left( \frac{C_k + C_{k+1}}{2} \right) (t_{k+1} - t_k)}{\sum_{k=1}^r \left( \frac{C_k + C_{k+1}}{2} \right) (t_{k+1} - t_k)} \quad (5b)$$

where  $k$  is an index and  $r$  is the total number of observations.

Using the continuous and uniform sampling that can be made available by *The Integrator* device, 0<sup>th</sup>-order temporal moments can be calculated from the final concentration of a single composite sample, which makes this technique ideal to perform inexpensive mass-balance analyses. Mathematically,

$$m_0 = \int_0^{t_f} C(t) dt = \tilde{C}_f t_f \quad (6a)$$

where  $\tilde{C}_f$  is the final, volume-averaged concentration collected in an initially (at  $t = 0$ ) empty bottle, after the continuous (from  $t = 0$  to  $t = t_f$ ), uniform sampling with *The Integrator* device is stopped at  $t = t_f$ . In general, the bottle does not have to be empty at  $t = 0$ , but the initial volume ( $V_0$ ) and concentrations ( $C_0$ ) of all the tracked dilution would need to be known to properly correct for dilution (i.e.,  $\tilde{C}_{f \text{ dilution}} = (\tilde{C}_f \cdot (V_f - V_0) + C_0 \cdot V_0) / V_f$ ; where  $V_f$  is the total volume inside *The Integrator's* bottle at time  $t_f$ ). Similarly, the concentrations of the tracer being monitored do not have to be zero at background conditions, but must be known to remove their effect

in the 0<sup>th</sup>-order temporal moment estimated with *The Integrator*, that is,

$$m_{0, \text{bckg-corrected}} = (\tilde{C}_f - \tilde{C}_{\text{fbckg}}) t_f \quad (6b)$$

where  $\tilde{C}_{\text{fbckg}}$  best represents pre- or postevent background concentrations, or their average. Alternatively, the term  $\tilde{C}_{\text{fbckg}} t_f$  can be replaced by the area under the curve of a function describing background variation over time, using the same methods used to remove baseflow in hydrograph analyses.

Note that for high-frequency, semi-continuous ( $\Delta t \rightarrow 0$ ) and uniform ( $\Delta t = \text{constant}$ ) monitoring:

$$m_0 = \int_0^{t_f} C(t) dt = \tilde{C}_{s-c} t_f \quad (7)$$

where  $\tilde{C}_{s-c}$  is the average of semi-continuous concentrations recorded by in situ sensors. In other words,  $\tilde{C}_f$  (from *The Integrator*, Eqs. 6a, 6b) and  $\tilde{C}_{s-c}$  (from semi-continuous sensors, Eq. 7) can be used interchangeably in all previous and upcoming equations. In the remainder of this article, we will use  $\tilde{C}_f$  in the formulae but recall that it could be changed to  $\tilde{C}_{s-c}$  if semi-continuous data are available.

The estimation of experimental 0<sup>th</sup>-order temporal moments with *The Integrator* device reduces costs and analytical times by a factor directly proportional to the number of samples that would have been collected (i.e., at least 20 per breakthrough curve in solute tracer experiments). Also, note that even though it would not be possible to directly estimate 1<sup>st</sup> order temporal moments (information on the time between the excitation and the characteristic response time of the flow system) from composite samples, *The Integrator* device could incorporate a sensor tracking the breakthrough curve of a conservative solute to compute  $m_1^*$  from Eq. 5b. This can be done using in-line microelectrodes reading out, for example, electrical conductivity or fluorescence as *The Integrator* samples. While not being able to estimate 1<sup>st</sup> order temporal moments directly from water samples seems to be a drawback of *The Integrator*, we show below that most of the metrics that are routinely estimated to characterize conservative and reactive transport can be calculated from 0<sup>th</sup>-order temporal moments and information that can be accurately approximated with readily available flow-trackers.

### ***The Integrator: Estimating reactivity in a river reach***

González-Pinzón and Haggerty (2013) developed an efficient method that can be used to estimate uptake (also referred to as decay, transformation, or processing) or production rate coefficients ( $\lambda$ ) using algebraic equations resulting from the 0<sup>th</sup>-order temporal moment of a solute transport model including advection, dispersion, transient-storage, and first-order decay (or production when  $\lambda < 0$  in Eqs. 8, 9). These

equations can be solved using upstream and downstream (superscripts up and dn below) experimental data gathered with *The Integrator*:

$$\lambda = \frac{\ln(m_{0,\text{reac.}}^{\text{up}}/m_{0,\text{reac.}}^{\text{dn}})}{uL} \left( 1 + \frac{\ln(m_{0,\text{reac.}}^{\text{up}}/m_{0,\text{reac.}}^{\text{dn}})}{Pe} \right) \quad (8)$$

where  $m_{0,\text{reac.}}^{\text{dn}} = m_0^{\text{dn}} (m_{0,\text{cons}}^{\text{dn}}/m_{0,\text{cons}}^{\text{up}})$  is the dilution corrected (inferred from a conservative tracer, subscript cons) 0<sup>th</sup>-order temporal moment of a reactive tracer;  $u$  the mean velocity in the reach ( $u = Q/A$ );  $A$  the cross-sectional area of the main channel;  $L$  the length of the reach;  $Pe = L u/D$  is the Peclet number, which describes the relative importance of advection and dispersion in the flow system; and  $D$  the dispersion coefficient. González-Pinzón and Haggerty (2013) demonstrated that for advection dominated systems, such as stream ecosystems,  $Pe > 100$  and this simplifies Eq. 8 to

$$\lambda_{Pe > 100} = \frac{\ln(m_{0,\text{reac.}}^{\text{up}}/m_{0,\text{reac.}}^{\text{dn}})}{uL} \quad (9)$$

Finally, the uptake (or production, if  $\lambda < 0$ ) length ( $S_w$ ) and uptake (or production, if  $\lambda < 0$ ) velocity ( $V_f$ ) metrics (see Ensign and Doyle 2006 for detailed descriptions of these metrics) can be calculated as:

$$S_w = \frac{u}{\lambda_{Pe > 100}} \quad (10)$$

$$V_f = \frac{Q/w}{S_w} \quad (11)$$

where  $w$  [L] is the average width of the stream reach. Briefly,  $S_w$  is the average distance traveled by a nutrient molecule prior to uptake and  $V_f$  is the average vertical velocity of nutrient molecules through the water column toward the most active uptake sites.

### **The Integrator: From mass-balances in a bottle to river processes**

For steady-flow conditions, the continuous, uniform sampling from *The Integrator* allows us to estimate mass-balance equations in a bottle (cf. Eqs. 6a, 6b) and extrapolate that knowledge to flow systems using simple scaling ratios, as Eq. 2 suggests. To demonstrate this, note that the final concentrations ( $\tilde{C}_f$ ) and 0<sup>th</sup>-order temporal moments ( $m_0 = \tilde{C}_f t_f$ ) that would be obtained from sampling continuously and uniformly an infinitesimal flowpath in a river would be the same that would be obtained if we divert all the flow crossing the same monitoring location and store it inside a nonleaking reservoir (infinite size bottle). Furthermore, for a conservative tracer, those equal 0<sup>th</sup>-order temporal moments would be equal to that at the injection point ( $m_{0\text{injection}} = M_{\text{inj}}/Q_{\text{@inj}}$ ;

where  $M_{\text{inj}}$  is the tracer mass injected and  $Q_{\text{@inj}}$  is the discharge at the injection location) if  $t_f$  is long enough to guarantee full mass recovery. Thus, the two seemingly distal sampling methods (infinitesimal flowpath vs. full-flow) follow one of Euclid's five axioms: "things which are equal to the same thing are equal to each other." Putting Euclid's axiom in the context of monitoring a conservative tracer following an instantaneous injection, the 0<sup>th</sup>-order temporal moments obtained with either the infinitesimal (continuous and uniform) or full-flow sampling approaches (or any alternative in between) are equal to  $m_{0\text{injection}}$  and, thus, equal to each other. Since  $q_{\text{Integrator}}$  is constant,  $M_{\text{Integrator}} = q_{\text{Integrator}} m_{0\text{Integrator}}$ , and then:

$$\begin{aligned} m_{0\text{injection}} = m_{0\text{Integrator}} &\rightarrow \frac{M_{\text{stream}}}{Q_{\text{stream}}} = \frac{M_{\text{Integrator}}}{q_{\text{Integrator}}} \\ &\rightarrow M_{\text{stream}} = \tilde{C}_f t_f Q_{\text{stream}} \end{aligned} \quad (12)$$

For unsteady flow conditions, Eq. 12 becomes:

$$M_{\text{stream}} = \int_{t=0}^{t=t_f} C(t) Q(t) dt \quad (13a)$$

$$M_{\text{stream}} = \sum_{k=1}^r \left( \frac{C_k + C_{k+1}}{2} \right) \left( \frac{Q_k + Q_{k+1}}{2} \right) (t_{k+1} - t_k) \quad (13b)$$

which can be used to analyze high-frequency sensor data. For composite sample with *The Integrator* device and for gradually varied flow,  $M_{\text{stream}}$  can be closely approximated by:

$$M_{\text{stream}} \sim \tilde{C}_f \int_{t=0}^{t=t_f} Q_{\text{stream}} dt \quad (13c)$$

$$M_{\text{stream}} \sim \tilde{C}_f \sum_{k=1}^r \left( \frac{Q_k + Q_{k+1}}{2} \right) (t_{k+1} - t_k) \quad (13d)$$

Note that Eqs. 12-13 can be used to estimate partial mass recoveries when  $t_f <$  time to full mass recovery, and that while any flow effects causing changes in the transport processes (e.g., advection, dispersion) and diluting the tracer signal will already be captured by  $\tilde{C}_f$ , Eq. 13 would only become an equality if the pumping rate of *The Integrator* device is directly proportional to the changes in discharge. Although this can be achieved, for example, by adjusting the pumping rate with a calibrated pressure transducer (i.e., using a known rating curve), it is likely that the uncertainty in the rating curve (typically ~10% or more) would be much greater than the error involved in the numerical approximation made in Eqs. 13c, 13d.

*The Integrator* sampling approach holds the associative property of addition and integration, meaning that the total 0<sup>th</sup>-order temporal moment equals the summation of 0<sup>th</sup>-order temporal moments captured by each of  $n$  bottles used during the experiment (i.e.,  $m_0 = \sum_{i=1}^n \tilde{C}_{f,i} t_{f,i}$ ). Also, while Eqs. 6a, 6b

do not impose limits on  $t_f$  from a practical standpoint the duration of the monitoring with *The Integrator* into a single bottle should be shorter than the time  $t_f$  for which  $\tilde{C}_f$  becomes smaller or near the limit of quantification of the analytical technique used to read the solute concentrations.

### **The Integrator: Estimating river discharges from instantaneous tracer injections**

*The Integrator* concepts can be applied to the well-documented salt dilution method of determining river discharge ( $Q$ ) under steady-state flow conditions (Kilpatrick and Cobb 1984). For this, a known mass of conservative tracer ( $M_{inj}$ ) needs to be injected and the experimental 0<sup>th</sup>-order temporal moment of the conservative tracer plume ( $m_{0Integrator}$ ) must be monitored at a location downstream of the lateral and vertical mixing zones. If there is not dilution between the injection and sampling sites,

$$Q = \frac{M_{inj}}{m_{0Integrator}} = \frac{M_{inj}}{\tilde{C}_f t_f} \quad (14)$$

### **The Integrator: Estimating steady-state gain or dilution factors**

The steady-state gain (SSG), or dilution factor within a reach, can be estimated using *The Integrator*. For this, a known mass of conservative tracer ( $M_{inj}$ ) is injected and the 0<sup>th</sup>-order temporal moment of the conservative tracer plume is monitored downstream of the lateral and vertical mixing zones:

$$SSG_{inj-dn} = \frac{m_{0Integrator}}{m_{0inj}} = \frac{\tilde{C}_f t_f}{M_{inj}} Q \quad (15)$$

Alternatively, two monitoring stations (upstream [up] and downstream [dn]) can be used to track the tracer plume and estimate SSG between them.

$$SSG_{up-dn} = \frac{m_{0Integrator}^{dn}}{m_{0Integrator}^{up}} = \frac{\tilde{C}_f t_f|_{dn}}{\tilde{C}_f t_f|_{up}} \quad (16)$$

## **Case studies**

### **Heart rate monitoring**

We used information from a heart rate monitoring device collecting data every second during running and biking workouts to validate *The Integrator* idea in a highly controlled experiment. We normalized the heart rate measurements by the maximum heart rate observed during each workout, which began at  $t = 0$  and ended at  $t_f$ . This controlled experiment offered data that, for practical purposes, were continuously and uniformly recorded, and represented the response (heart rate variability) of a system (person) to known perturbations

(workouts). Using the experimental data, in Fig. 1 we present the results of: (1) using Eq. 5a to estimate the experimental 0<sup>th</sup>-order temporal moment from all the data recorded (3600 measurements per hour of workout), (2) comparing those numbers with the calculations derived from *The Integrator* concept (Eq. 7), and (3) analyzing the effects of adding data gaps lasting 1, 3, and 5 min to compare differences between “continuous” and semi-continuous, but still uniform monitoring.

### **Field tracer experiments**

#### **Site descriptions**

##### *Fourth-order stream*

We conducted an instantaneous tracer injection experiment in the Jemez River, NM (U.S.A.) to compare results from manual grab sampling, semi-continuous sensor data, and sampling with *The Integrator* (Fig. 2). The Jemez River is a tributary of the Rio Grande and drains approximately 1450 km<sup>2</sup> of the Jemez Mountains in north-central New Mexico. Mean annual discharge is 1.4 m<sup>3</sup> s<sup>-1</sup> (2004–2015, USGS gauge #08324000). Downstream of our study reach, the Jemez continues for approximately 50 km until it reaches the Rio Grande. Table 2 summarizes relevant information from this tracer experiment. For the Jemez experiment, we injected and monitored NaCl as a conservative tracer, and resazurin and NaNO<sub>3</sub> as reactive tracers.

##### *Seventh-order stream*

We conducted another instantaneous tracer injection experiment in the Rio Grande, near Albuquerque, NM (U.S.A.). We injected and monitored NaBr as a conservative tracer and NaNO<sub>3</sub> as a reactive tracer in a 7<sup>th</sup> order river reach affected by populated areas, flow control dams, and agricultural diversion dams. Mean annual discharge in the study reach is ~ 25 m<sup>3</sup> s<sup>-1</sup> (2004–2015, USGS gauge #08329918). Table 2 summarizes relevant information from this tracer experiment, and we note that between the injection and the sampling sites, there is an agricultural diversion channel that changed flow from 8.9 to 7.4 m<sup>3</sup> s<sup>-1</sup> (Fig. 2).

#### **Monitoring and analytical methods**

The timing for manual grab sample collection was guided by a predictive model simulating solute transport conditions for the in-stream characteristics presented in Table 2 and by in situ sensor measurements. These samples were taking at the thalweg of the stream using triple rinsed syringes and filtered immediately using 0.45 μm nylon filters (Whatman). For the semi-continuous monitoring, we deployed YSI EXO2 sondes measuring nitrate (NO<sub>3</sub>, using an ion-selective electrode), temperature and specific conductivity, an S::Can probe tracking NO<sub>3</sub> (spectrophotometric detection) and a SUNA V2 probe tracking NO<sub>3</sub> (spectrophotometric detection). The YSI sondes measured every 30 s and the dedicated NO<sub>3</sub> sensors every 2 min.

*The Integrator* device (see Supporting Information) sampled at each sampling location using a pump pulling water into an off-line (hydraulically disconnected) container that vacuum-filtered

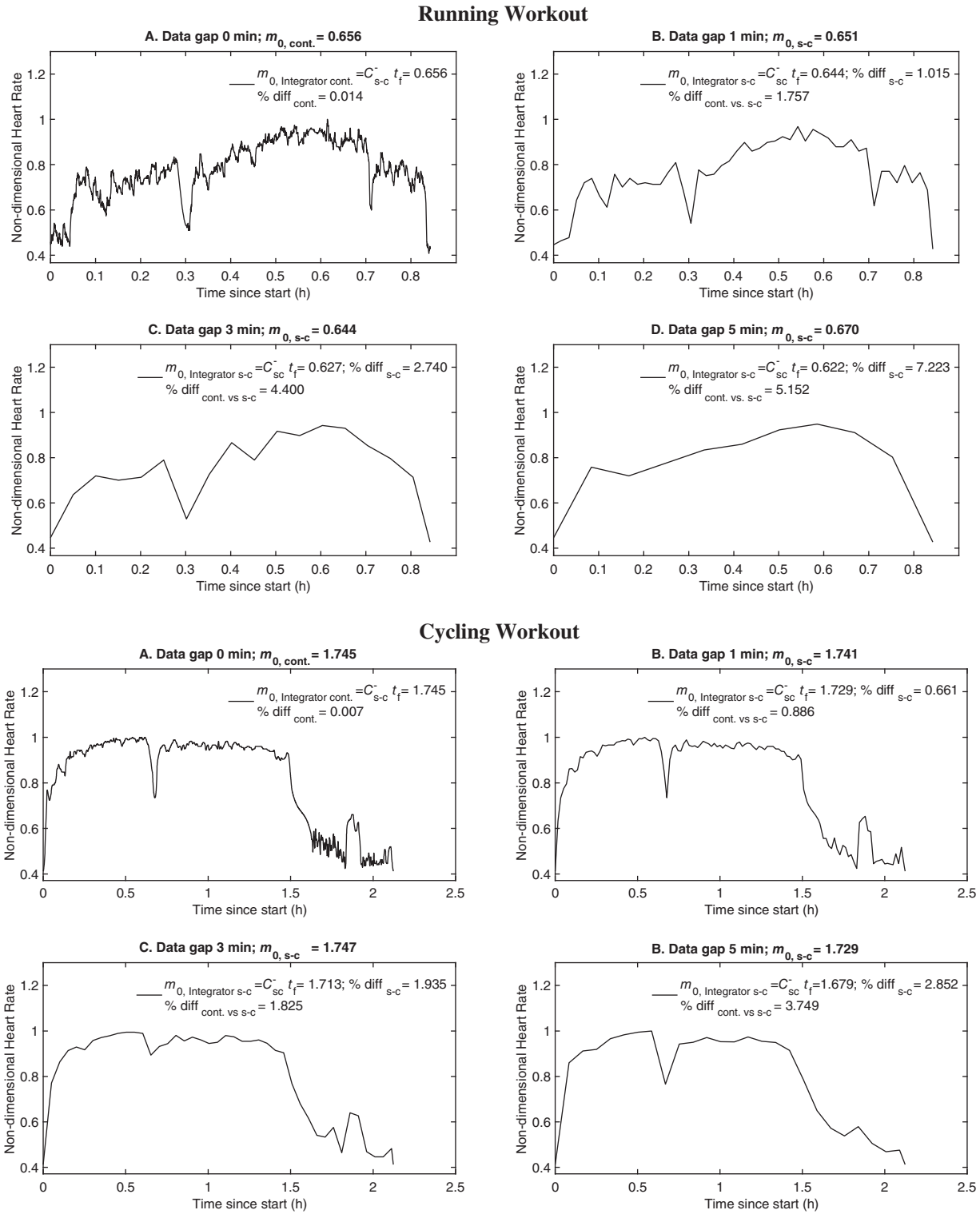


**Fig. 1.** *The Integrator*: Concept validation using heart rate data from two workouts. **(A)** Original data recorded every second (continuous monitoring, referred to as “cont.”). **(B–D)** Resampling representative of heart rate data collected every minute **(B)**, every 3 min **(C)**, and every 5 min **(D)** (semi-continuous monitoring, referred to as “s-c”).  $\% \text{diff}_{\text{cont.}} = 100 \cdot \text{abs}[(m_{0, \text{Integrator cont.}}/m_{0, \text{cont.}}) - 1]$  is the percent difference between estimating  $m_0$ , the 0<sup>th</sup>-order experimental temporal moment, with Eq. 5a (trapezoidal integration with all data available) and Eq. 7 ( $m_{0, \text{Integrator}} = \bar{C}_{s-c} t_f$ ; *The Integrator* concept);  $\% \text{diff}_{s-c} = 100 \cdot \text{abs}[(m_{0, \text{Integrator s-c}}/m_{0, \text{s-c}}) - 1]$  and  $\% \text{diff}_{\text{cont. vs s-c}} = 100 \cdot \text{abs}[(m_{0, \text{Integrator s-c}}/m_{0, \text{cont.}}) - 1]$  are estimated for each gap treatment.





**Fig. 2.** (Left) Jemez River (4<sup>th</sup> order stream). (Right) Rio Grande (7<sup>th</sup> order stream) and diversion channel.

**Table 2.** Field tracer experiment characteristics.

	Masses injected			Sampling locations		Average flow characteristics		
	NaCl or NaBr (g)	Resazurin (g)	NaNO <sub>3</sub> (g)	Upstream (US) (m)	Downstream (DS) (m)	Discharge (m <sup>3</sup> s <sup>-1</sup> )	Width (m)	Depth (m)
4 <sup>th</sup> order	5896	50	1000	910	1665	0.254	4.5	0.3
7 <sup>th</sup> order	31,062	N/A	36,475	N/A	5665	8.215	27.5	0.61

N/A = Not applicable.

the water through a multifilter system with minimum pore size of 0.45  $\mu\text{m}$ , and then placed the water into the final storage bottle. The prototype of the Integrator device used was selected after early tests indicated that the most accurate continuous and uniform sampling could be achieved when the pumping lines were hydraulically disconnected from any component creating backpressures. Additional details about construction of *The Integrator* device can be found in the Supporting Information. All manual grab and *Integrator* samples were stored on ice in the field, during transport, and in storage, and were analyzed within 3 d of collection. Chloride (Cl), bromide (Br), and nitrate (NO<sub>3</sub>) samples were analyzed using a Dionex ICS-1000 Ion Chromatograph with AS23/AG23 analytical and guard columns. Resazurin samples were analyzed using a Varian Carry Eclipse spectrofluorometer, following the methods described in Knapp et al. (2018).

#### Comparison of 0<sup>th</sup>-temporal moments and transport metrics

We used Eqs. 5a, 6b to independently estimate background-corrected 0<sup>th</sup> temporal moments from manual grab samples,

sensor data, and *The Integrator* samples (Table 3). Using manual grab sampling as the correct, most established method, we computed relative differences in estimating 0<sup>th</sup> temporal moments with data derived from sensors and *The Integrator* (e.g., %diff. =  $100 \cdot \text{abs}[(m_{0, \text{Integrator}}/m_{0, \text{grab}}) - 1]$ ).

We used Eqs. 9–11 (based on 0<sup>th</sup> temporal moments) to estimate uptake metrics for the reactive tracers resazurin and NO<sub>3</sub> (Table 4). Since uptake rate coefficients ( $\lambda$ ) are used to estimate the uptake length ( $S_w$ ) and uptake velocity ( $V_p$ ) metrics, and are a function of the 0<sup>th</sup> temporal moments in Table 3, we used the differences between 0<sup>th</sup> temporal moments in Table 3 to estimate minimum-maximum ranges for each uptake metric, instead of reporting single values. In doing this, we seek to better understand the uncertainty of the uptake metrics with respect to likely numerical errors caused from analytical (e.g., limits of detection) or integration (e.g., truncation) approximations. For example, the ranges shown in Table 4 for the resazurin uptake metrics estimated from both manual grab and *The Integrator* samples consider



**Table 3.** Comparison of 0<sup>th</sup>-temporal moments estimated with data from field tracer experiments. US, upstream; DS, downstream;  $m_0$ , 0<sup>th</sup> temporal moment.

Jemez River 4 <sup>th</sup> order	Cl		Resazurin		NO <sub>3</sub>	
	$m_0$ (mg min L <sup>-1</sup> )	%diff.	$m_0$ (mg min L <sup>-1</sup> )	%diff.	$m_0$ (mg min L <sup>-1</sup> )	%diff.
US manual grab	241.2	—	12.8	—	46.2	—
US sensor	N/A		N/A		49.2	6.5
US integrator	234.8	2.7	12.4	3.2	46.5	0.6
DS manual grab	233.6	—	11.0	—	40.0	—
DS sensor	N/A		N/A		40.1	0.2
DS integrator	234.8	0.5	11.4	3.8	42.5	6.2

Rio Grande 7 <sup>th</sup> order	Br		No resazurin injected		NO <sub>3</sub>	
	$m_0$ (mg min L <sup>-1</sup> )	%diff.	$m_0$ (mg min L <sup>-1</sup> )	%diff.	$m_0$ (mg min L <sup>-1</sup> )	%diff.
DS manual grab	55.7	—	N/A		58.7	—
DS sensor	N/A				59.5	1.3
DS integrator	60.2	7.9			58.0	1.1

N/A = Not applicable.

**Table 4.** Comparison of uptake metrics based on 0<sup>th</sup> temporal moments estimated with data from field tracer experiments. US, upstream; DS, downstream;  $m_0$ , 0<sup>th</sup> temporal moment.  $\lambda$ ,  $S_w$ , and  $V_f$  are the uptake rate coefficients, uptake lengths, and uptake velocities.

	$\lambda$ (min <sup>-1</sup> )	$S_w$ (m)	$V_f$ (m min <sup>-1</sup> )	$\lambda$ (min <sup>-1</sup> )	$S_w$ (m)	$V_f$ (m min <sup>-1</sup> )
<b>Jemez River 4<sup>th</sup> order</b>		<b>Resazurin</b>			<b>NO<sub>3</sub></b>	
US to DS manual grab	$1.4 \times 10^{-5}$ to $3.1 \times 10^{-5}$	$3.6 \times 10^5$ to $7.8 \times 10^5$	$4.3 \times 10^{-6}$ to $9.4 \times 10^{-6}$	$1.3 \times 10^{-5}$ to $3.0 \times 10^{-5}$	$3.7 \times 10^5$ to $8.2 \times 10^5$	$4.1 \times 10^{-6}$ to $9.1 \times 10^{-6}$
US to DS sensor		N/A		$4.0 \times 10^{-5}$ to $5.6 \times 10^{-5}$	$2.0 \times 10^5$ to $2.7 \times 10^5$	$1.2 \times 10^{-5}$ to $1.7 \times 10^{-5}$
US to DS integrator	$1.7 \times 10^{-6}$ to $1.9 \times 10^{-5}$	$5.9 \times 10^5$ to $6.6 \times 10^6$	$5.1 \times 10^{-7}$ to $5.7 \times 10^{-6}$	$2.8 \times 10^{-6}$ to $1.9 \times 10^{-5}$	$5.7 \times 10^5$ to $3.9 \times 10^6$	$8.5 \times 10^{-7}$ to $5.9 \times 10^{-6}$
<b>Rio Grande 7<sup>th</sup> order</b>		<b>No resazurin injected</b>			<b>NO<sub>3</sub></b>	
DS manual grab		N/A		$3.0 \times 10^{-6}$ to $3.6 \times 10^{-6}$	$8.3 \times 10^6$ to $1.0 \times 10^7$	$2.0 \times 10^{-6}$ to $2.4 \times 10^{-6}$
DS sensor				$8.1 \times 10^{-7}$ to $1.1 \times 10^{-6}$	$2.7 \times 10^7$ to $3.7 \times 10^7$	$5.3 \times 10^{-7}$ to $7.3 \times 10^{-7}$
DS integrator				$1.2 \times 10^{-6}$ to $2.6 \times 10^{-6}$	$1.1 \times 10^7$ to $2.4 \times 10^7$	$8.2 \times 10^{-7}$ to $1.7 \times 10^{-6}$

N/A = Not applicable.

the between method variability of the 0<sup>th</sup> temporal moments ( $\pm 3.2\%$  and  $\pm 3.8\%$  at the upstream and downstream sites, respectively), as reported in Table 3.

Using Eq. 12, background corrected samples, and the uncertainty propagation framework explained above, we estimated ranges for the masses recovered at our upstream and downstream sampling sites (Table 5). Our results successfully demonstrate the applicability of the mathematical framework linking mass balances in a bottle to the understanding of in-stream processes. We developed this framework while

developing *The Integrator*, but its formulae are transferable to any sampling technique including grab and semi-continuous sampling techniques (see “*The Integrator: From mass-balances in a bottle to river processes*” section).

## Discussion and conclusions

*The Integrator* is a novel technique to monitor environmental systems. Its development resulted in two products: (1) *The Integrator* device, which we briefly described in the

**Table 5.** Comparison of masses recovered based on 0<sup>th</sup> temporal moments estimated with data from field tracer experiments. US, upstream; DS, downstream;  $m_0$ , 0<sup>th</sup> temporal moment.

Masses recovered (g)						
Jemez River 4 <sup>th</sup> order	Cl 3577 g injected		NO <sub>3</sub> 730 g injected		Resazurin 50 g injected	
	US	DS	US	DS	US	DS
	Grab	3577–3772	3539–3577	700–708	572–648	48–51
Sensor	N/A		701–798	610–613	N/A	
Integrator	3482–3672	3558–3596	704–712	607–688	46–49	42–45
Rio Grande 7 <sup>th</sup> order	Br 31,062 g injected		NO <sub>3</sub> 36,475 g injected		No resazurin injected	
	DS	DS, with diversion	DS	DS, with diversion		
	Grab	27,664–32,420	22,932–26,874	29,539–30,219	24,486–25,050	N/A
Sensor	N/A		31,642–32,468	26,228–32,468		
Integrator	29,854–34,986	24,747–29,001	30,930–31,643	25,639–26,230		

N/A = Not applicable.

“Monitoring and analytical methods” section and further explain in detail in the Supporting Information, and (2) the mathematical framework presented in the “Conceptual and mathematical framework” section. The use of *The Integrator* device simplifies sample collection and greatly reduces the number of samples needed to quantify conservative and reactive transport metrics commonly used in the study of flow systems, resulting in considerable cost and time savings. We demonstrated that the mathematical framework that we developed to support *The Integrator* device as an improved, grab sampling technique is also compatible with semi-continuous monitoring. This is ideal to reconcile and contrast data gathered with different techniques across continents. Due to the practicality, simplicity, and precision offered by *The Integrator*, we envision that this technique will increase the number of environmental studies in understudied regions, where taking one or a few sample(s) with high-information content is not just the only affordable or tractable option, but also one that can empower researchers and practitioners to start to or better understand mechanistic processes. This advancement will also be valuable for researchers studying highly instrumented sites by allowing them to directly correlate known excitation events (e.g., tracer injections and natural or anthropogenic disturbances) with system responses captured by established sensor data. Here, we discuss the results of our case studies and then expand in detail on a variety of potential uses and advances made possible by *The Integrator*.

### Proof of concept and validation from field studies

#### Heart rate monitoring

The highly controlled experiments using heart rate data from two workouts successfully proved the concept behind *The*

*Integrator* (Fig. 1). Specifically, the differences caused by using  $m_{0, \text{Integrator cont.}} = \tilde{C}_{s-c} t_f$  (Eq. 7) instead of  $m_{0, \text{cont.}}$  from Eq. 5a were less than 0.01% for the continuous (every second) time-series (see %diff<sub>cont.</sub> in Fig. 1A), less than 7.2% for the semi-continuous (1, 3, and 5 min data gap) time-series (see %diff<sub>s-c</sub> in Fig. 1B–D), and less than 5.2% when continuous and semi-continuous time-series were compared (see %diff<sub>cont. vs. s-c</sub> in Fig. 1B–D). In general, the %diff increased with increasing data gaps but even the largest data gaps (5 min) kept the 0<sup>th</sup> order temporal moments estimated within 10% difference for all calculations performed using these highly dynamic time-series. Thus, our analyses validate a key concept: continuous, uniform sampling can be used to simplify mass-balance characterizations. This type of sampling can be achieved with *The Integrator* device (see Supporting Information) and is intrinsically available in semi-continuous sensors.

#### Field studies

The results from our field studies in two contrasting rivers (4<sup>th</sup> and 7<sup>th</sup> order) in New Mexico validated the applicability of *The Integrator* device and the mathematical framework that supports it. In our comparisons between the results generated from manual grab sampling, which was assumed as the reference method, and *The Integrator* device and semi-continuous sensors, we found differences that for all practical purposes can be deemed negligible, particularly knowing the limitations of manual grab sampling (Drummond et al. 2012). Specifically, the 0<sup>th</sup>-temporal moments estimated with data from field tracer experiments had percent differences (%diff) < 8% for both conservative and reactive tracers (Table 3). Moreover, the estimates of the masses recovered (Table 5) were consistent with the masses injected and the transport and reaction processes expected to occur along the study reaches.

Our analyses to validate *The Integrator* suggest that the logarithmic function describing uptake/production rate coefficients in common transport models (e.g., advection-dispersion-reaction and transient storage models, cf. Eqs. 9–11) amplify relatively small differences in 0<sup>th</sup> temporal moments. Here, we exemplify the sensitivity of the amplification of errors in estimating metrics that rely on 0<sup>th</sup> temporal moments by assuming that their magnitudes at upstream and downstream locations are 2.5 and 2.0 (arbitrary units). For these numbers, the numerator in Eq. 9 (uptake rate coefficients), which would be the changing quantity in the ratio, is  $\ln(2.5/2.0) = 0.1$ . Next, if we add a  $\pm 5\%$  difference or uncertainty to each of the two 0<sup>th</sup>-order temporal moments, the numerators will range from 0.05 to 0.14, with percent differences in the estimated metrics of up to 46%. In general, the percent difference in the evaluation of the uptake rate coefficient grows with the percent difference in the estimated 0<sup>th</sup> temporal moments, and also with their similarity (i.e., the percent difference increases in reaches with little reaction). This simple numerical sensitivity analysis demonstrates the importance of reporting uptake metrics as ranges (cf. Table 4), accounting for uncertainty in their estimates, instead of single values. We argue that too often the numerical sensitivity behind uptake (or related) metrics is overlooked and that this oversight hinders intersite or interseason comparisons. The uncertainties in estimating 0<sup>th</sup>-order temporal moments increase when: (1) there are missing samples in the tail of the breakthrough curve and/or the limits of quantification do not allow long-tail tracking, (2) there are outliers, (3) sensors drift, and/or (4) background correction is made difficult by diurnal cycles in the monitored solutes. Thus, *The Integrator* could also be used to take low-cost replicate samples at a given location to provide more accurate estimates of nutrient uptake parameters which we now know are highly susceptible to slight errors.

### Benefits and potential uses of the integrator

A primary benefit of *The Integrator* technique is that it reduces the cost and analytical times required for the estimation of experimental 0<sup>th</sup>-order temporal moments by a factor directly proportional to the number of samples that were previously required to collect a time-series during a typical field monitoring campaign. From our own experience, at least 20 samples are typically required for the collection of one concentration breakthrough curve in solute tracer experiments. These savings are particularly important for research that requires a significant degree of spatial, temporal, or experimental replication. For example, the authors are currently using *The Integrator* to estimate nutrient uptake rates for 64 replicate hyporheic mesocosms. Using previous methods, these experiments would have generated approximately 1300 samples and have cost approximately USD \$13,000 and over 530 h of ion chromatography run-time to analyze (assuming USD \$10 and 25 min per sample). Instead, using *The Integrator*, similar information content will be obtained with 1/20<sup>th</sup> of the cost and time.

In another research project, we are currently conducting monthly, multiyear tracer experiments in select reaches located along a 1<sup>st</sup>–8<sup>th</sup> river order fluvial network. While we have sensors monitoring forms of C, N, and P, and proxies for conservative transport (e.g., specific conductivity and stage), they cannot uniquely relate observed nutrient concentrations with nutrient uptake metrics. Thus, we are conducting repetitive tracer experiments in contrasting river reaches to develop a robust framework capable of linking semi-continuous nutrient concentrations with transport and reactive processes over the range of natural discharge conditions observed. To exemplify our approach, let us contrast the pairing of repetitive tracer injections and semi-continuous monitoring of concentrations with the monitoring of glucose in a (pre)diabetic patient. While glucose levels (or nutrient concentrations in streams) let us quantify if the patient is glucose impaired (or eutrophic), those measurements alone do not provide mechanistic information on how the patient's body (or stream system) assimilates sugars, carbohydrates, and nutrients (or C and nutrients). Only until we relate food intake (or known C and nutrient loading in tracer experiments) with observed glucose and nutrient levels (or resulting breakthrough curve concentrations), will we understand how external forcing functions combine with the natural system to produce the results that we can monitor (glucose or concentration levels). This analogy clearly suggests the need for replicate estimates of uptake metrics over contrasting flow and watershed conditions, a need which *The Integrator* is helping us meet.

The previously high cost of measuring solute breakthrough curves in lotic systems has prevented researchers from collecting nutrient uptake data at the same frequency as lower cost measurements. For example, the current generation of dissolved oxygen probes produces low cost, high quality, and frequency data, and can be deployed in flowing systems for long periods. This has allowed lotic researchers to calculate near-continuous estimates of whole stream gross primary production and ecosystem respiration (Stanley and del Giorgio 2018; Bernhardt et al. 2018), which are important measures of ecosystem function. These data are providing new insights into the temporal dynamics of stream ecosystem function and how this function responds to disturbance. To date, the high cost of nutrient uptake experiments has prevented pairing metabolism data with high frequency nutrient uptake data, obscuring relationships between these important measures of ecosystem function. *The Integrator* will thus help researchers studying highly instrumented sites gain key mechanistic understanding by allowing them to directly correlate known excitation events (e.g., tracer injections and natural or anthropogenic disturbances) with system responses captured by established sensor data. Additionally, as lower cost and higher resolution near-continuous nutrient sensors become available, the mathematical framework that supports *The Integrator* provides an analytical tool to estimate and compare nutrient uptake

parameters, independently of whether the data come from grab or semi-continuous data.

In addition to increasing the potential frequency of nutrient and solute uptake measurements, *The Integrator* will also allow researchers to estimate these parameters at broader spatial scales. A first example of the problematic status quo with respect to the spatial scale of sampling is that in spite of long theorized longitudinal differences in nutrient processing along the river continuum (Vannote et al. 1980; Creed et al. 2015), the vast majority of experimental work has focused on head-water streams (Tank et al. 2008; Hall et al. 2013). This bias reflects the difficulty of sampling in large rivers and has generated fundamental knowledge gaps regarding the mechanistic behavior of nutrient dynamics across fluvial networks. Second, it is becoming well known that there is a disproportionate concentration of scientific studies in the Northern Hemisphere, despite the ecohydrological importance of intertropical and low-latitude ecosystems for local-to-planetary biogeochemical cycles (Riveros-Iregui et al. 2018). Clearly, this spatial research gap resembles larger-scale socioeconomic disparities. Since, to date, and for the foreseeable future, the number of environmental researchers and practitioners that have the possibility to choose whether to use semi-continuous or grab sampling (or both) in their monitoring likely represents the immense minority, we need to develop new knowledge that can help us simplify and improve both grab and semi-continuous monitoring. Through our personal experience submitting proposals and research articles that have benefitted from, and have been challenged by, the use of both monitoring techniques (Mortensen et al. 2016; Knapp et al. 2018; Riveros-Iregui et al. 2018), we have perceived an unnecessary predilection for semi-continuous monitoring. We believe that such cultural bias is not only unnecessary, as both grab and semi-continuous monitoring are known to have shortcomings and benefits, but also harmful because it may inadvertently contribute to increase the knowledge gap between more studied regions, where still only some research groups can afford semi-continuous sensors, and other understudied locations that may hold high information content about environmental processes. Thus, making grab and semi-continuous sampling analogous when monitoring the same system (i.e., same location, time and solutes) will provide more equal opportunities for researchers across the planet and will also greatly improve scientific reproducibility and allow meaningful comparisons between highly instrumented and ungauged sites. Simply put, *imagine the frivolous alternative fate of humanity had Charles Darwin done all his research just in England, even with unlimited access to what was considered cutting-edge technology in his days!*

Despite our case studies focused on the analysis of conservative and reactive transport of solutes in rivers, the principles behind *The Integrator* technique can be used to monitor water quality in hyporheic zones, aquifers, wetlands, swamps, karsts, oceans, wastewater treatment plants, pipe networks, and even

air quality. Furthermore, special arrangements of *Integrator* devices can be used to gather data at spatial and temporal resolutions that are currently unattainable due to high transportation and/or personnel costs. Finally, as described in the Supporting Information, *The Integrator* can be used to pioneer the next generation of remote monitoring, where a smart system operated remotely via telemetry activates both a dispenser releasing known quantities of tracer salts and *The Integrator* sampling device.

## References

- Bayard, D., M. Stähli, A. Parriaux, and H. Flühler. 2005. The influence of seasonally frozen soil on the snowmelt runoff at two Alpine sites in southern Switzerland. *J. Hydrol.* **309**: 66–84. doi:[10.1016/j.jhydrol.2004.11.012](https://doi.org/10.1016/j.jhydrol.2004.11.012).
- Berkowitz, B., and H. Scher. 1995. On characterization of anomalous dispersion in porous and fractured media. *Water Resour. Res.* **31**: 1461–1466. doi:[10.1029/95WR00483](https://doi.org/10.1029/95WR00483).
- Bernhardt, E. S., and others. 2018. The metabolic regimes of flowing waters. *Limnol. Oceanogr.* **63**: S99–S118. doi:[10.1002/lno.10726](https://doi.org/10.1002/lno.10726).
- Creed, I. F., and others. 2015. The river as a chemostat: Fresh perspectives on dissolved organic matter flowing down the river continuum. *Can. J. Fish. Aquat. Sci.* **72**: 1272–1285. doi:[10.1139/cjfas-2014-0400](https://doi.org/10.1139/cjfas-2014-0400).
- Cunningham, J. A., and P. V. Roberts. 1998. Use of temporal moments to investigate the effects of nonuniform grain-size distribution on the transport of sorbing solutes. *Water Resour. Res.* **34**: 1415–1425. doi:[10.1029/98WR00702](https://doi.org/10.1029/98WR00702).
- Das Bhabani, S., Rao S. Govindaraju, J. Kluitenberg Gerard, J. Valocchi Albert, and M. Wraith Jon. 2013. Theory and applications of time moment analysis to study the fate of reactive solutes in soil. In *Stochastic methods in subsurface contaminant hydrology*. ASCE Press.
- Drummond, J. D., T. P. Covino, A. F. Aubeneau, D. Leong, S. Patil, R. Schumer, and A. I. Packman. 2012. Effects of solute breakthrough curve tail truncation on residence time estimates: A synthesis of solute tracer injection studies. *J. Geophys. Res. Biogeosci.* **117**: G00N08. doi:[10.1029/2012JG002019](https://doi.org/10.1029/2012JG002019).
- Ensign, S. H., and M. W. Doyle. 2006. Nutrient spiraling in streams and river networks. *J. Geophys. Res. Biogeosci.* **111**: G04009. doi:[10.1029/2005JG000114](https://doi.org/10.1029/2005JG000114).
- Goeury, C., J.-M. Hervouet, I. Baudin-Bizien, and F. Thouvenel. 2014. A Lagrangian/Eulerian oil spill model for continental waters. *J. Hydraul. Res.* **52**: 36–48. doi:[10.1080/00221686.2013.841778](https://doi.org/10.1080/00221686.2013.841778).
- González-Pinzón, R., and R. Haggerty. 2013. An efficient method to estimate processing rates in streams. *Water Resour. Res.* **49**: 6096–6099. doi:[10.1002/wrcr.20446](https://doi.org/10.1002/wrcr.20446).
- González-Pinzón, R., R. Haggerty, and M. Dentz. 2013. Scaling and predicting solute transport processes in streams. *Water Resour. Res.* **49**: 4071–4088. doi:[10.1002/wrcr.20280](https://doi.org/10.1002/wrcr.20280).

- González-Pinzón, R., J. Mortensen, and D. Van Horn. 2015. Comment on “Solute-specific scaling of inorganic nitrogen and phosphorus uptake in streams” by Hall et al. (2013). *Biogeosciences* **12**: 5365–5369. doi:[10.5194/bg-12-5365-2015](https://doi.org/10.5194/bg-12-5365-2015).
- Govindaraju, R. S., and B. S. Das. 2007. Moment analysis for subsurface hydrologic applications. Springer.
- Hall, R. O., Jr., M. A. Baker, E. J. Rosi-Marshall, J. L. Tank, and J. D. Newbold. 2013. Solute-specific scaling of inorganic nitrogen and phosphorus uptake in streams. *Biogeosciences* **10**: 7323–7331. doi:[10.5194/bg-10-7323-2013](https://doi.org/10.5194/bg-10-7323-2013).
- Harvey, C. F., and S. M. Gorelick. 1995. Temporal moment-generating equations: Modeling transport and mass transfer in heterogeneous aquifers. *Water Resour. Res.* **31**: 1895–1911. doi:[10.1029/95WR01231](https://doi.org/10.1029/95WR01231).
- Kilpatrick, F. A., and E. D. Cobb. 1984. Measurement of discharge using tracers. U.S. Geological Survey, Report 84–136.
- Knapp, J. L. A., R. González-Pinzón, and R. Haggerty. 2018. The resazurin-resorufin system: Insights from a decade of “smart” tracer development for hydrologic applications. *Water Resour. Res.* **54**: 6877–6889. doi:[10.1029/2018WRO23103](https://doi.org/10.1029/2018WRO23103).
- Kraus, T. E. C., K. O'Donnell, B. D. Downing, J. R. Burau, and B. A. Bergamaschi. 2017. Using paired in situ high frequency nitrate measurements to better understand controls on nitrate concentrations and estimate nitrification rates in a wastewater-impacted river. *Water Resour. Res.* **53**: 8423–8442. doi:[10.1002/2017WR020670](https://doi.org/10.1002/2017WR020670).
- Leube, P. C., W. Nowak, and G. Schneider. 2012. Temporal moments revisited: Why there is no better way for physically based model reduction in time. *Water Resour. Res.* **48**: W11527. doi:[10.1029/2012WRO11973](https://doi.org/10.1029/2012WRO11973).
- Melcher, A. A., and J. S. Horsburgh. 2017. An urban observatory for quantifying phosphorus and suspended solid loads in combined natural and stormwater conveyances. *Environ. Monit. Assess.* **189**: 285. doi:[10.1007/s10661-017-5974-7](https://doi.org/10.1007/s10661-017-5974-7).
- Mortensen, J. G., R. González-Pinzón, C. N. Dahm, J. Wang, L. H. Zeglin, and D. J. Van Horn. 2016. Advancing the food-energy–water nexus: Closing nutrient loops in arid river corridors. *Environ. Sci. Technol.* **50**: 8485–8496. doi:[10.1021/acs.est.6b01351](https://doi.org/10.1021/acs.est.6b01351).
- Nordin, C. F., and G. V. Sabol. 1974. Empirical data on longitudinal dispersion in rivers. USGS numbered series 74–20. U.S. Geological Survey.
- Riveros-Iregui, D. A., T. P. Covino, and R. González-Pinzón. 2018. The importance of and need for rapid hydrologic assessments in Latin America. *Hydrol. Process.* **32**: 2441–2451. doi:[10.1002/hyp.13163](https://doi.org/10.1002/hyp.13163).
- Schmid, B. H. 2003. Temporal moments routing in streams and rivers with transient storage. *Adv. Water Resour.* **26**: 1021–1027. doi:[10.1016/S0309-1708\(03\)00086-1](https://doi.org/10.1016/S0309-1708(03)00086-1).
- Schumer, R., M. M. Meerschaert, and B. Baeumer. 2009. Fractional advection-dispersion equations for modeling transport at the Earth surface. *J. Geophys. Res.* **114**: F00A07. doi:[10.1029/2008JF001246](https://doi.org/10.1029/2008JF001246).
- Stanley, E. H., and P. A. del Giorgio. 2018. Toward an integrative, whole network approach to C cycling of inland waters. *Limnol. Oceanogr.: Lett.* **3**: 39–40. doi:[10.1002/lol2.10085](https://doi.org/10.1002/lol2.10085).
- Tank, J. L., E. J. Rosi-Marshall, M. A. Baker, and R. O. Hall. 2008. Are rivers just big streams? A pulse method to quantify nitrogen demand in a large river. *Ecology* **89**: 2935–2945. doi:[10.1890/07-1315.1](https://doi.org/10.1890/07-1315.1).
- Vannote, R. L., G. W. Minshall, K. W. Cummins, J. R. Sedell, and C. E. Cushing. 1980. The river continuum concept. *Can. J. Fish. Aquat. Sci.* **37**: 130–137. doi:[10.1139/f80-017](https://doi.org/10.1139/f80-017).
- Vaughan, M. C. H., and others. 2017. High-frequency dissolved organic carbon and nitrate measurements reveal differences in storm hysteresis and loading in relation to land cover and seasonality. *Water Resour. Res.* **53**: 5345–5363. doi:[10.1002/2017WRO20491](https://doi.org/10.1002/2017WRO20491).
- Wlostowski, A. N., M. N. Gooseff, W. B. Bowden, and W. M. Wollheim. 2017. Stream tracer breakthrough curve decomposition into mass fractions: A simple framework to analyze and compare conservative solute transport processes. *Limnol. Oceanogr.: Methods* **15**: 140–153. doi:[10.1002/lom3.10148](https://doi.org/10.1002/lom3.10148).
- Zhang, R., K. Huang, and M. T. van Genuchten. 1993. An efficient Eulerian-Lagrangian Method for solving solute transport problems in steady and transient flow fields. *Water Resour. Res.* **29**: 4131–4138. doi:[10.1029/93WR01674](https://doi.org/10.1029/93WR01674).
- Zhang, Y., M. M. Meerschaert, B. Baeumer, and E. M. LaBolle. 2015. Modeling mixed retention and early arrivals in multidimensional heterogeneous media using an explicit Lagrangian scheme. *Water Resour. Res.* **51**: 6311–6337. doi:[10.1002/2015WRO16902](https://doi.org/10.1002/2015WRO16902).

## Acknowledgments

After a concept development of “The Integrator” by R. González-Pinzón, the products presented in this manuscript were part of a class project in the CE 598 Ecohydrology graduate course taught by R. González-Pinzón at the University of New Mexico. We thank Julia Knapp for her comments on a draft of this manuscript, and the reviewers and editors involved in the peer-review process. The National Science Foundation provided funding support to the graduate students and postdoc Peter Regier through grants CBET-1707042, HRD-1345169, HRD-1720912, EAR-1642399, and DGE-1418062. This material is also based upon work supported by the U.S. Department of Energy, Office of Science, Office of Biological & Environmental Research, under Award Number DE-SC0019424.

## Conflict of Interest

None declared

Submitted 30 January 2019

Revised 13 May 2019

Accepted 23 May 2019

Associate editor: Clare Reimers